JAST, Vol. 7, No. 2, pp 131–137

JAST
Journal of Aerospace Science and Technology

Wind Tunnel Investigation of Pressure Distribution and Transition Position of a Swept 3D Wing

M. Soltani[1], M. Masdari[2], M. Seidjafari[3], K. Ghorbanian[4]

Several extensive wind tunnel tests were conducted to evaluate surface pressure distribution of a semi span swept wing. The wing section had a laminar flow airfoil similar to NACA 6-series airfoils. The investigations were conducted at various speeds and angles of attack. Surface pressure distribution over the wing upper surface is measured for both chordwise and spanwise sections. The relevant statistical analyses were performed on the data to realize the transition point at each chordwise section. The 3D pressure profiles were compared to the corresponding 2D results under the same conditions. Calculation of the standard deviation, SD, of time variable pressure data showed that SD increases in the transition area and then decreases again when the flow becomes fully turbulent downstream. The measured transition points were further compared with 2D computational results.

NOMENCLATURE

V_∞	Freestream velocity (m/sec)
C_p	Pressure coefficient= $\frac{p-p_\infty}{q_\infty}$
P_∞	Wind tunnel static pressure
q_∞	Dynamic pressure= $\frac{1}{2}\rho_\infty V_\infty^2$(N/m^2)
ρ_{infty}	Air density (kg/m^3)
Re	Reynolds number= $\frac{\rho_\infty V_\infty C}{\mu}$
C	Airfoil chord (m)
C_r	Wing root chord (m)
C_t	Wing tip chord (m)
$\bar{C}$	Wing average chord = $\frac{C_t+C_r}{2}$ (m)
μ	Air viscosity

Abbreviation

AOA	Angle of attack (degree)
SD	Standard deviation

1. *Professor, Dept. of Aerospace Eng., Sharif Univ. of Tech., Tehran, Iran, Email: msoltani@sharif.edu.*
2. *Ph.D. Candidate, Dept. of Aerospace Eng., Sharif Univ. of Tech., Tehran, Iran, Email: mmasdari@sharif.edu.*
3. *M.Sc. Graduate, Dept. of Aerospace Eng., Sharif Univ. of Tech., Tehran, Iran, Email: seidjafari@sharif.edu.*
4. *Professor, Dept. of Aerospace Eng., Sharif Univ. of Tech., Tehran, Iran, Email: Ghorbanian@sharif.edu.*

INTRODUCTION

Prandtl (1914) deduced that the flow in the boundary layer could become turbulent and early transition to turbulence could be trigged by surface roughness. Further, he hypothesized that first a turbulent boundary layer has a higher skin friction drag and second separation is delayed when the boundary layer is turbulent. Thus, for a bluff body, the drag is reduced when the separation is delayed and is usually achived by trigging the transition point. However, for a streamline body, *i.e.* an airfoil, where the drag is mainly due to skin friction, a delay of the transition to turbulence will reduce the drag. Tollemien (1929) and Schlichting (1933) were able to theoretically determine the critical Reynolds number of the transition point for the boundary layer over a flat plate. Further, the transition point can be pushed back by furnishing a smooth surface. These finding led to the development of laminar flow airfoils by Jacob (1939) and others at NACA. The corresponding airfoils had significantly lower drag coefficients when compared to the earlier ones. Subsequently, methods for predicting the critical Reynolds number, the extent of the transition zone,

and laminar separation and reattachment were innovated [1].

When a laminar flow airfoil is employed in a 3D wing, some of its characteristics like pressure profiles, boundary layer transition point, *etc.* are changed. Hence, these variations are of great importance and must be predicted prior to their flight tests.

Boundary layers over swept wing, yawed cylinders, or at junctions of two bodies are three dimensional in nature. Flow measurements in these areas are very challenging. Van den berg & Elsenaar (1972) have reported flow measurements on an infinite swept wing. They have further reported pressure distribution, velocity profiles, and turbulent stresses. Spaid *et.al.* (1990) presented measurements on models of transport aircraft, *i.e.* their wing-body combination. Information of the skin friction drag is a special feature of their data.

An experimental study was conducted on F-14A at Langley Research Center in 1989 to investigate the transition point variable sweep wings modified for laminar flow. The tests revealed the influence of cross-flow (CF) and Tollmein-Schlichting (TS) instabilities on the boundary layer transition and showed the effect of wing sweep on the boundary layer transition point [2].

Allthough a considerable number of experimental and theoretical studies have been performed with respect to transition point, as stated above, the surface pressure distribution, transition point, and other characteristics of an airfoil still vary when it is employed in a wing. Therefore, for a specific wing, one must evaluate the aforementioned variables by using CFD and performing experiments. Due to the lack of information on employment of airfoil in a wing, the authors have decided to perform some experiments to pinpoint the transition point. It is anticipates that the experimental data in conjunction with CFD results would help to better predict the behavior of the original model. Hence, the present paper describes the flow field over a 3D wing as well as the surface pressure distribution at various angles of attack. The reported data are from experiment performed in a subsonic wind tunnel.

EXPERIMENTAL APPARATUS

All experiments were conducted in a subsonic wind tunnel of closed return type with a test section of 80cm×80cm×200cm operating at speeds from 10 to 100 m/sec. The inlet of the tunnel has a 7:1 contraction ratio with four large, anti-turbulence screens and a honeycomb in its settling chamber to reduce the tunnel turbulence to less than 0.1 percent in the test section.

The model used in this experiment is a scaled model of a tapered wing whose section is similar to that of NACA6-series airfoil. A half model was designed and fabricated to achieve higher Re number during the tests. A flat plate was used at the end of the model to reduce the boundary layer effect of the test section on the model.

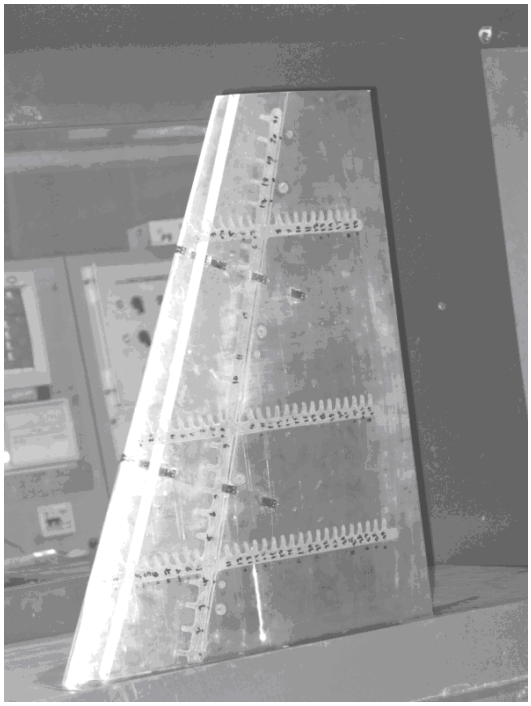

Figure 1. Model installed in the wind tunnel.

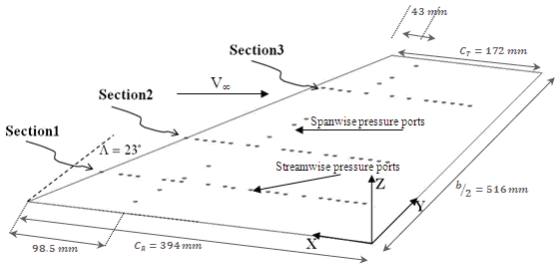

Figure 2. Schematic of the test setup and pressure orifices on the wing surface.

The general arrangement of the model used for this investigation when installed in the wind tunnel is shown in Figure 1. The baseline configuration is a semi-span, a 1/2.5 scale model of the actual wing. The model has a leading edge sweep of 23° and a span of 516mm. The wing's upper surface is covered with 90 pressure orifices of 0.4 mm diameter arranged in three streamwise rows, section 1 through section 3, and one spanwise section at 1/4 chord line, Figure 2.

All pressure data are collected via an accurate pressure transducer. Data are collected via a terminal board and transmitted to the computer through a 64 channel, 12-bit Analog-to-Digital (A/D) board capable of an acquisition rate of up to 500 kHz. Raw data are then digitally filtered using a low-pass filtering routine.

Furthermore, using the method explained in Ref. 3, both the single sample precision and the bias uncertainty in each measured variable were estimated and then they were propagated into the C_P variations. The maximum overall uncertainty calculated in this way for the C_P data was less than ±3% of the total C_P values.

RESULTS AND DISCUSSIONS

Visualization

The flow visualization over the upper surface of the wing was performed by using mini fluorescent tufts and ultra violet ray. Visualization tests show that at all speeds, and for angles of attack up to 10°, the flow remains attached over the entire wing surface, Figure 3a & b. However, a few tufts indicate of detached flow over the wing surface when the angle of attack was increased to 12°, Figure 4. These tufts were mainly located in the vicinity of the leading edge near the wing tip. It is believed that this separation is due to the bubble that forms in the leading edge which is similar to the mechanism of the stall for the NACA 6 series airfoils, Figure 4. The flow over the wing was fully separated when the AOA was increased to $\alpha = 18°$, Figure 5. As seen from Figure 5, almost all tufts behave chaotically which is an indication of the separated flow. The stalled area in Figure 5 is shown by a rectangle drown through the tufts.

Furthermore, it is seen that for this wing, the flow separation occurs in the vicinity of the mid span and moves toward the tip. The tufts near the root chord remaine attached to the surface even at 18° angle of attack, Figure 5. Chaotic motions of the tufts in the leading edge area may indicate that the bubble has burst for this angle of attack.

Visualization tests were conducted to distinguish the transition area, but unfortunately the tests did not reveal the transition point because the tuft diameter was not in the order of the boundary layer thickness.

Surface Pressure Results

Static pressure over the wing's upper surface at all stations, station 1 through station 3, are shown in Figure 2. The model is instrumented with three chordwise rows of pressure orifices located at the inboard section of the wing, section 1 ($y/b = 0.2$ outboard section), section 2 ($y/b = 0.43$ middle section), and section 3 ($y/b = 0.78$ outboard station), Figure 2. The tests were conducted at tunnel speeds of V_∞=50-80 m/s and at angles of attack ranging from α=-2 to 8 degrees. Figure 6 shows the effect of angle of attack on the wing surface pressure distribution for the middle section, section 2. It can be seen by inspection that as the angle of attack increases, a suction peak over the wing surface for the section under study is developed. For angles of attack of α=4 to 6 degrees, the peak pressure located at $\frac{x}{c} \cong 0.05$ moves toward the leading edge, $\frac{x}{c} \cong 0$ for higher AOA, $\alpha = 7°$ and 8°, Figure 6. Note that the area over the wing surface where $\frac{dC_P}{dx}$ is negative is called favorable pressure gradient region and the value of C_p increases negatively creating more suction over the wing surface. For the positive pressure gradient region, $\frac{dC_p}{dx} > 0$, $|C_p|$ decreases but the value of C_p increases positively and is called adverse pressure gradient.

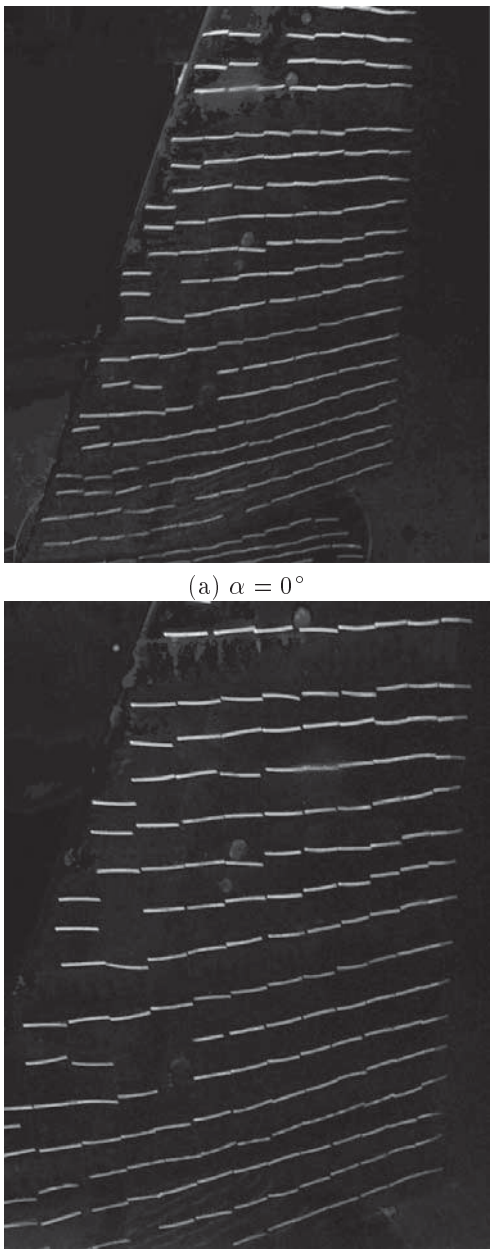

(a) $\alpha = 0°$

(b) $\alpha = 11°$

Figure 3. Fluorescent tuft flow visualization at V=50 m/s.

For angles of attack $3 \leq \alpha \leq 8°$, the flow over the wing surface after the suction peak encounters a region of adverse pressure gradient and continues until the wing trailing edge. However, the slope of C_p over the

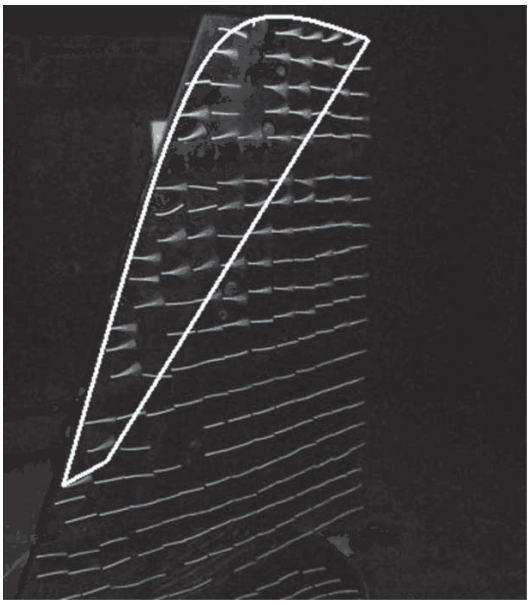

Figure 4. Fluorescent tuft flow visualization at V=50m/s, $\alpha = 18^\circ$.

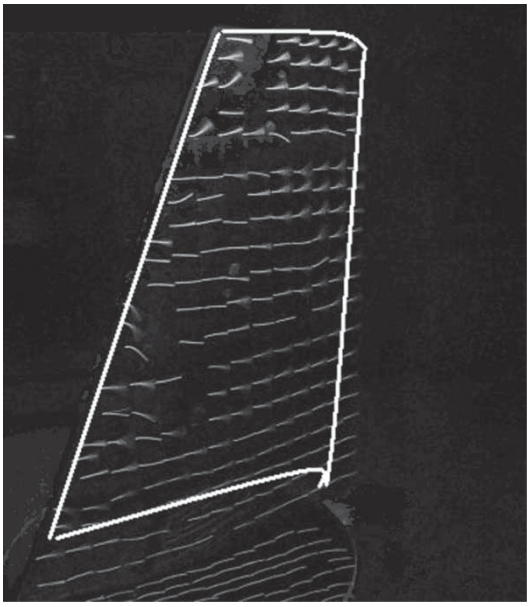

Figure 5. Fluorescent tuft flow visualization at V=50 m/s, $\alpha = 18^\circ$.

wing surface varies as seen from Figure 6. For angles of attack of 2 and 3 degrees, the suction peak on the C_p data cannot be distinguished. Figure 6 shows that for these angles of attack, $|C_p|$ increases from $x/c = 0$ to $x/c \cong 0.04$ and then remains almost constant up to $x/c \cong 0.045$, a region of almost constant pressure, $\frac{dC_p}{dx} \cong 0$. For $x/c > 0.45$, the flow encounters a region of adverse pressure gradient for $\alpha = 2$ and 3 degrees where $|C_p|$ decreases. The C_p data for other angles of attack, $-2 \leq \alpha \leq 0$ degrees, show that the flow over the wing's upper surface accelerates from $x/c = 0$ to $x/c \cong 0.048$ and then decelerates over the rest of the wing surface, $x/c > 0.48$. From these data, it could be concluded that the flow over a significant portion of the wing surface remains laminar if the wing is flying at angles of attack of zero to 3 degrees. However, it should be mentioned that the existence of a low suction peak in the leading edge vicinity for $\alpha = 3^\circ$, seen in Figure 6, may trigger the boundary layer transition; *i.e.* transition may occur closer to the leading edge.

For higher angles of attack, specially $\alpha > 6^\circ$, the existence of a large suction peak in the vicinity of the wing leading edge indicates that the flow will become turbulent close to the suction peaks, $x/c > 0$. From the surface pressure data, it is seen that the flow will be definitely transient to turbulence between $0 < x/c < 0.15$ for angles of attacks of 7 and 8 degrees.

The flow over the wing surface at this section, section 2, seems to be completely attached for all angles of attack shown in this figure which is in agreement with the visualization photo as shown in Figure 3. In addition to the C_p data shown in Figure 6, the error corresponding to the measured data is shown for one C_p point. The calculated error is around 3% of the full scale.

Figures 7 and 8 show the effect of Reynolds number on the wing surface pressure at section 2 for two different angles of attack, $\alpha = 0^\circ$ and $\alpha = 8^\circ$. It should be noted that the Reynolds number in this tunnel is varied by changing the free stream velocity. This method will change the flow compressibility; however, since the maximum free stream velocity is $V_\infty = 80m/s$, the aforementioned effect is negligible. From these figures, it is clearly seen that these Reynolds numbers do not have a significant influence on the wing surface pressure distribution.

The comparison between different stations for a free stream velocity of 50 m/sec and at two different

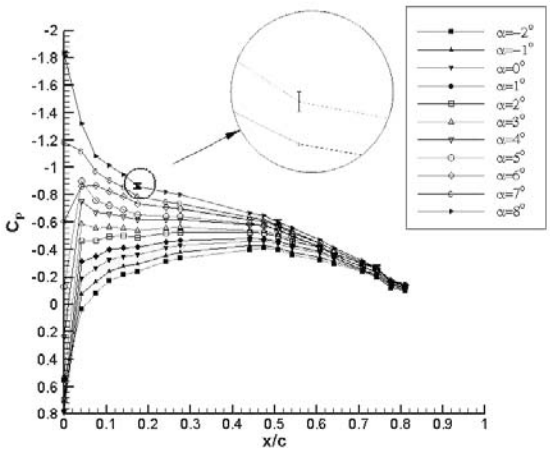

Figure 6. Effect of A.O.A on the chordwise pressure distribution, section 2 at v= 50 m/s.

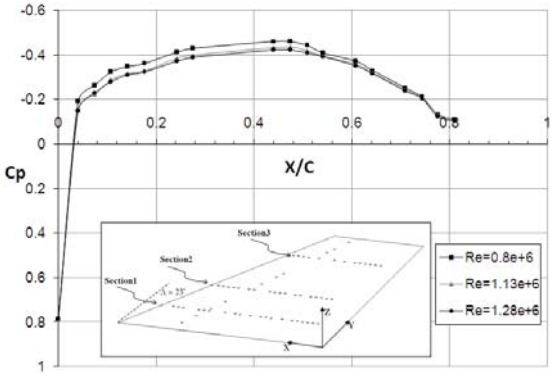

Figure 7. Pressure distribution over section 2 at various Re, $\alpha = 0°$.

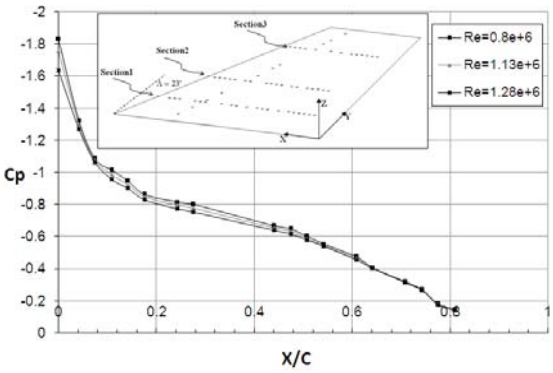

Figure 8. Pressure distribution over section 2 at various Re, $\alpha = 8°$.

angles of attack, $\alpha = 0°$ and $\alpha = 5°$, is shown in Figure 9. From these data, it is seen that different wing sections are not affected by the wing body conjunction (in the inner section) and wing tip vortex (in the outer station) seriously, at least for these two angles of attack. However, for the 5 degree angle of attack, Figure 9 shows that the C_p in the vicinity of the wing leading edge differs slightly for each section, *i.e.* suction peaks for all 3 sections do not occur at the same x/c and their absolute values, $|C_p|$, are not the same either. However, for $x/c > 0.2$, the C_p data for all 3 sections are identical, Figure 9b.

When an airfoil is employed in a wing, some of its characteristics like pressure profiles and the transition point at different stations will change. For an untwisted swept wing with a similar airfoil section the loading is concentrated towards the tip. In addition, both root and tip effects reduce the isobars in a direction normal to the flow, Ref. [4], so that the sectional pressure profile of a 3D wing will be different from that of the 2D airfoil pressure profile of the same geometry. Comparison of the Eppler data [5] with those of the present experiment, Figure 9a, shows good agreement for section 2, middle section, at $\alpha = 0°$. As the angle of attack is increased, Figure 9b, the differences between the panel method C_p distributions obtained from the Eppler code and the experimental data increase too. It should be pointed out that the Eppler data are for a 2D airfoil and the effect of three dimensionality is not considered. These differences are related to the growth of 3D effect, the strength of wing tip vortex, and body effect as well as the wing sweep on modifying the flow stream lines over the wing surface. In addition, from Figure 9b, it is evident that the clearest difference between the Eppler data and the experimental results occurs in the vicinity of the wing leading edge, $0 \leq x/c \leq 0.4$. For $x/c > 0.4$, experimental results and Eppler data do not differ significantly. This may indicate that all the effects mentioned above are mainly concentrated near the wing leading edge, at least for the angle of attack considered in this study. Further, the data reveal that when an airfoil is employed in a wing, a drastic change may occur in its suction peak which may be both advantageous and disadvantages. The advantage is demonstrated by the disappearance of the suction peak, as seen from the data of Figure 9b, indicating that the transition will be definitely postponed to higher x/c's values. It should be mentioned that high suction peak with enhance the transition toward the leading edge and should be avoided in airfoil designs. However, decreasing the suction peaks will reduce the sectional C_l value and consequently the overall wing lift will

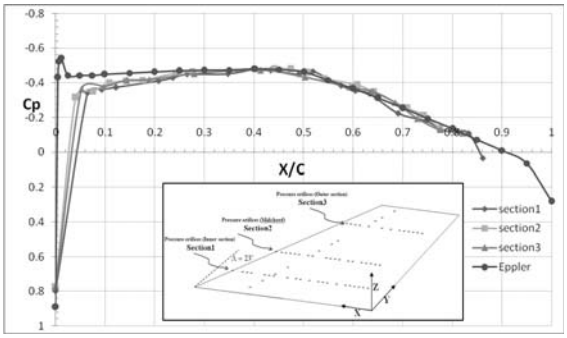

(a) $\alpha = 0°$

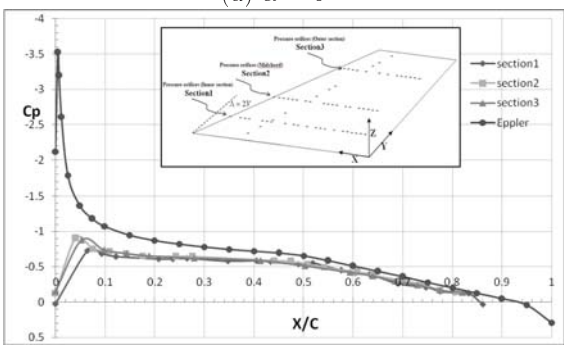

(b) $\alpha = 5°$

Figure 9. Pressure distribution over various sections of the wing at V=50 m/s.

be reduced which could be counted as a drawback for an aircraft. For further pressure profiles at different angles of attack over different wing sections, the reader is referred to Ref. [6].

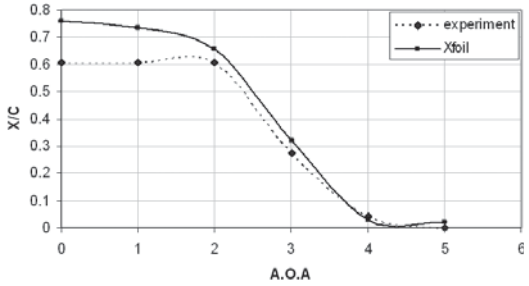

Figure 11. Comparison of the predicted transition point from the S. D. data with the X-foil code for section 2, V_∞ = 50 m/sec.

Transition Detection

It is well known that, in the transition region, the disorder of the flow eddies is more than that of other regions, *i.e.* laminar or turbulent ones. Studies of the statistical property of the pressure signals can be used to approximately identify the transition limits. Standard deviation parameter is a suitable factor to indicate the level of flow disorder. In the transition region, the value of this parameter increases sharply and decreases again where the flow becomes turbulent [7]. The changes in the standard deviation parameter are shown in Figures 10a-d for pressure ports located at station 2, chordwise middle station, and for four different angles of attack. As seen from Figure 10a, the SD parameter for the pressure port located at $\frac{x}{c} \cong 0.6$ of section 2 is maximum. Accordingly, this location is in the vicinity of the transition region. This is clearly in agreement with the C_p data shown on the top of Figure 10a. It should be taken into consideration that the C_p data for this station and for $\alpha = 0$ degree decreases

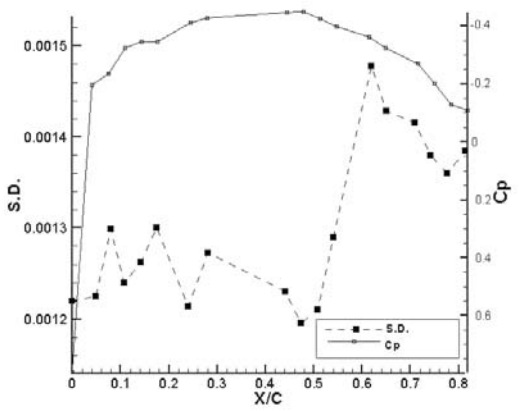

(a) $\alpha = 0°$

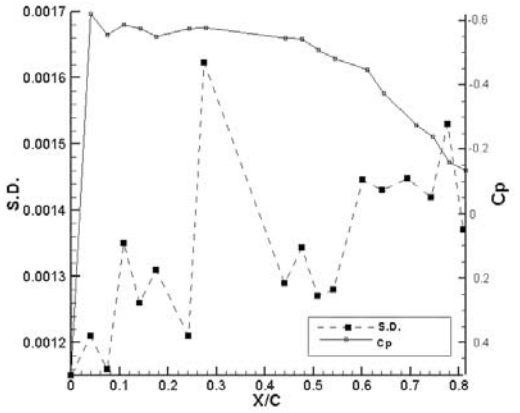

(b) $\alpha = 3°$

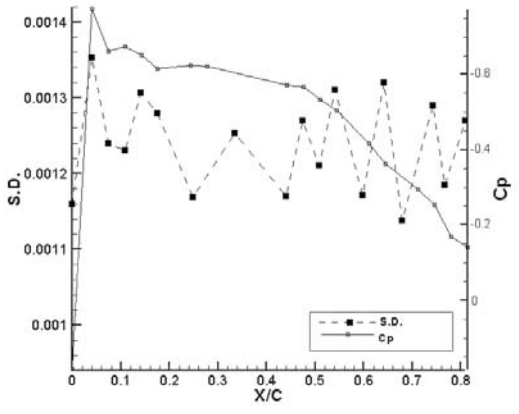

(c) $\alpha = 4°$

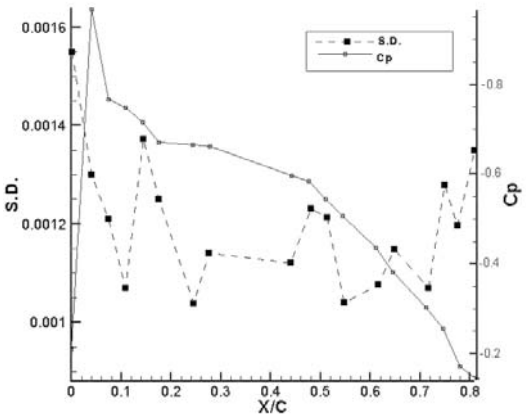

(d) $\alpha = 5°$

Figure 10. Variations of the standard deviation and C_p with x/c for section 2, V_∞ = 50 m/sec.

from the wing leading edge up to $x/c = 0.48$ which definitely indicates a laminar boundary layer. However, in the adverse pressure gradient region, $x/c > 0.48$, the flow still remains laminar for a distance, *i.e.* it resists to become turbulent. In this region, $0.48 < x/c \leq 0.6$, the flow in its transition state and, as seen from Figure 10a, the SD increases drastically. When the angle of attack is increased to $\alpha = 3°$, Figure 10b, the maximum SD occurs at $\frac{x}{c} \cong 0.3$ indicating that the small suction peak in the C_p data near the leading edge is responsible for triggering the transition. From the C_p data, it is seen that C_p for this angle of attack decreases up to $\frac{x}{c} \cong 0.48$, but the SD data show that the transition occurs even before this point. This is the main reason that one should avoid having suction peak in the C_p data as much as possible. This shows that by increasing the AOA, the transition region moves toward the wing leading edge. However, from Figures 10c and 10d, where the model is set to AOA of 4 and 5 degrees respectively, it is seen that variations of the SD with $\frac{x}{c}$ are random. Therefore, it is deduced that for these angles of attack, the flow over the entire model at this section is turbulent, and is clearly verified by the C_p data, *i.e.* suction peak in the vicinity of the leading edge has triggered an early transition.

Finally, variations of the boundary layer transition point with an angle of attack is shown in Figure 11 based on the previous figures. As it is evident, the flow over a significant portion of the wing surface for section 2 remains laminar up to an angle of attack of $\alpha \cong 2°$. By further increasing the AOA, the turbulent flow moves forward and covering the entire wing surface at $\alpha \cong 4°$. This type of transition movement is a key characteristic of the laminar flow airfoils. In Figure 11, the position of the transition point calculated by the X-Foil code [8] is shown for comparison. The experimental transition point is seen to be closer to the wing leading edge when compared to theoretical prediction of the X-foil code which could be due to the 3D effect and instability modes. It should be pointed out that the calculated transition point from the X-Foil code is for 2D airfoil and is mostly based on semi-empirical methods. Furthermore, it might be possible for the wing sweep angle to form instability modes like the crossflow mode that promote transition phenomena.

CONCLUSION

A number of experiments were performed to measure the pressure distribution on the upper surface of a 3D wing. The obtained results were compared with the corresponding 2D values for the same condition. From the static pressure data the boundary layer transition was obtained. Section pressure profiles showed deviation from the 2D predicted values. It is believed that the crossflow which originates from the finite aspect ratio and sweep angle of the wing is responsible for these deviations. Statistical studies on the standard deviation of the time variable pressure data were used to distinguish an estimation of the transition point over the wing surface and the results were in good agreement with those obtained from the C_p data. Finally, the comparison of the predicted transition point via statistical SD with those of the 2D values from the X-Foil code showed good agreement except for very low angles of attack.

ACKNOWLEDGMENTS

The authors would like to thank the staff of the Jahad Research Center for being allowed to use the wind tunnel. In addition, the financial support of the design bureau of Iran Aircraft Iindustries & Manufacturing (HESA) is greatly appreciated.

REFERENCES

1. Tulapurkara E.D., "Hundred Year of the Boundary Layer-Some Aspects", *Sadhana*, **30**(4), (2007).
2. Hallissy B.J., Philips S.P., "Wind-Tunnel Investigation of Aerodynamic Characteristics and Wing Pressure Distribution of an Airplane With Variable-Sweep Wings Modified for Laminar Flow", Langley research center, Hampton, Virginia, (1989).
3. Thomas G.B., Roy D.M. and John H.L.V., *Mechanical Measurements*, Addison-Wesley Publishing Company, (1993).
4. Raymer P.D., *Aircraft Design: A Conceptual Approach*, Third Edition, AIAA Education Series, (1999).
5. Eppler R., and Somers D.M., "A Computer Program for the Design and Analysis of Low-Speed Airfoils", *NASA TM 80210*, (1980).
6. Agha seidjafari M., "Experimental Study of the Wing Sweep Angle Effect on the Pressure Distribution of a Half Model", M.S. Thesis, Aerospace Engineering Department, Sharif University of Technology, (2009).
7. Kachanov Y.S., "Experimental Studies of Three-Dimentional Boundary Layers", *AIAA Paper 96-1978*, (1996).
8. Drela M., "An Analysis and Design System for Low Reynolds Number Airfoils", *Conference on Low Reynolds Number Airfoil Aerodynamics*, University of Notre Dame, (1989).